

Tracking Control of Quadrotor Based on Robust Adaptive Fuzzy Nonsingular Fast Terminal Sliding Mode with parameter uncertainties

Journal Title
XX(X):1–11
©The Author(s) 2016
Reprints and permission:
sagepub.co.uk/journalsPermissions.nav
DOI: 10.1177/ToBeAssigned
www.sagepub.com/



Hujie Wei and Yan Jiang

Abstract

Unknown disturbances, actuator saturation, or time-varying parameters negatively affect the tracking performance of the quadrotor. This paper proposes a robust adaptive fuzzy nonsingular fast terminal sliding mode controller (RAFNFTSMC) to solve the tracking problem. The arctangent nonsingular terminal sliding surface is selected to shorten convergence time for tracking errors. An improved reaching law accelerates convergence speed in sliding arrival phase. Furthermore, the adaptive fuzzy approximation not only eliminates the impact of parameter uncertainty, but also diminishes the chattering of the sliding mode. Moreover, an adaptive anti-saturation method efficiently handles the actuator saturation which occurs in real flight. System stability is validated by the Lyapunov direct method. The simulation results suggest that the RAFNFTSMC method improves robustness and convergence speed compared with similar plans. Finally, two sets of comparative studies about control precision and chattering magnitude show the outstanding performance of the proposed method.

Keywords

Quadrotor, chattering, fuzzy approximation, parameter uncertainty, actuator saturation

Introduction

Quadrotor Unmanned Aerial Vehicle (UAV) is a flexible, miniature aircraft. The application of quadrotor has become the focus of many engineers because it can perform complex tasks such as rescue, counter-terrorism, transportation, etc^{1,2}. But the features such as under-driven, high-coupling pose a difficulty for controller design of the quadrotor. To cope with the above problem, many researchers have proposed nonlinear control methods such as backstepping³, fuzzy-gain sliding mode control⁴, adaptive methods⁵, ADRC⁶. One of the most suitable methods for quadrotor is sliding mode control due to its features of the insensitivity to unknown disturbances and parameter uncertainties⁷. Furthermore, a compound sliding mode controller has achieved remarkable results^{8–10}.

An adaptive fuzzy terminal sliding mode control is proposed by Nekoukar et al¹¹. The adaptive fuzzy method is used to identify the quadrotor unknown functions online, the PD controller controls the attitude and horizontal position, and the continuous terminal sliding mode is defined to eliminate chattering. Oliva-Palomo F et al.¹² proposed a quadrotor attitude control method based on a fractional-order PI nonlinear structure. The method ensures the regularity of the control signal can be adjusted according to the fractional order. An adaptive super-twisting terminal sliding mode control method is proposed with the input delay, model uncertainty and wind disturbances¹³. The unknown bounds of model uncertainty and wind disturbance are estimated using the adaptive tuning control law. Xu LX et al.¹⁴ divided the quadrotor controller design into two steps. The attitude subsystem is decomposed into two serial-connected

subsystems using cascade active disturbance rejection, and the position loop is controlled using backstepping sliding mode control. An adaptive fast non-singular terminal sliding mode controller is proposed by Lian S et al¹⁵. The scheme integrates the advantages of integral sliding mode, non-singular terminal sliding mode, and adaptive estimation to weaken chattering and achieve fast tracking.

Inspired by previous researches, a robust adaptive fuzzy nonsingular fast terminal sliding mode controller (RAFNFTSMC) is proposed in this paper. The proposed RAFNFTSMC method ensures high accuracy, fast response, and robustness for tracking problem of quadrotor subjected to actuator saturation and parameter uncertainties. By using arctangent nonsingular terminal sliding surface, finite convergence time can be accomplished for errors. Considering the quadrotor physical parameters are unmeasurable or time-varying, the fuzzy approximation is employed to estimate the attitude controllers and switching functions in position-loop. The adaptive method is used to compensate an upper bound on the approximation error of the fuzzy system. Besides, many studies ignore actuator saturation, it is of practical importance that we estimate unknown saturation errors online using adaptive anti-saturation to handle actuator saturation. Lastly, two sets of simulations verify the

School of Electrical Engineering, Guangxi University, Nanning, 530004, China.

Corresponding author:

Yan Jiang, School of Electrical Engineering, Guangxi University, No.100, Daxuedong Road, Xixiangtang District, Nanning, 530004, China.
Email: yanjiang986@126.com

effectiveness and robustness of the proposed method. The contributions are summarized as follows:

(1) Distinct from some works^{16,17}, the proposed method fully considers various uncertainties, random noise and actuator saturation.

(2) Compared with the existing scheme^{4,18}, an arctangent nonsingular terminal sliding surfaces is firstly designed to realize finite time convergence.

(3) Unlike work from Wang N et al³, The fuzzy approximation eliminates the effect of uncertainty and suppresses chattering.

(4) The adaptive method estimates unknown errors regarding to fuzzy systems and actuator saturation.

The rest of this article is arranged as follows: The quadrotor dynamics model is provided in section “Problem formulation”. “Controller design” describes the proposed RAFNFTSMC scheme. The simulation results and comparison with similar methods are presented in Section “Simulation results”. Section “Conclusion” makes a summary.

Problem formulation

The quadrotor used in this paper is a cross-type quadrotor. The structure of the quadrotor is shown in Fig. 1. Four motors drive the quadrotor to move and rotate. Two assumptions are given as follows:

Assumption 1. Quadrotors are homogeneous rigid bodies.

Assumption 2. Quadrotor flies in small attitude angles.

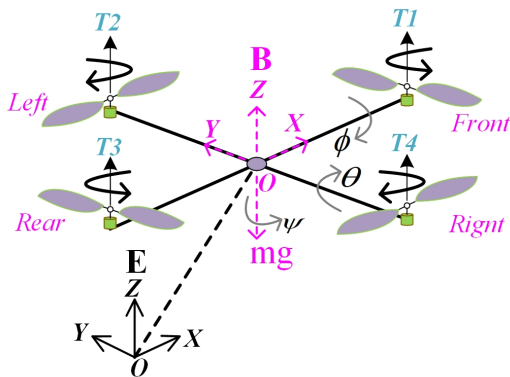


Figure 1. Structure of the quadrotor.

Define the earth-frame as $\mathbb{E} = \{x_e, y_e, z_e\}$ and define the body-frame as $\mathbb{B} = \{x_b, y_b, z_b\}$. The attitude angles associated with the earth-frame is $\xi = [\phi, \theta, \psi]^T$, $\phi \in (-\frac{\pi}{2}, \frac{\pi}{2})$, $\theta \in (-\frac{\pi}{2}, \frac{\pi}{2})$, $\psi \in (-\pi, \pi)$ and $\varsigma = [x, y, z]^T$ defines the position in earth-frame. The rotation matrix $R_{\mathbb{B} \rightarrow \mathbb{E}}$ is used to describe the coordinate transformation and its expression is:

$$R_{\mathbb{B} \rightarrow \mathbb{E}} = \begin{bmatrix} c\theta c\phi & s\theta c\phi s\psi - c\psi s\phi & c\phi s\theta c\psi + s\phi s\psi \\ c\theta s\phi & s\theta s\phi s\psi + c\psi c\phi & c\phi s\theta s\psi - c\psi s\phi \\ -s\theta & s\psi c\theta & c\phi c\theta \end{bmatrix} \quad (1)$$

where $c(*) = \cos(*)$ and $s(*) = \sin(*)$, for $* \in \phi, \theta, \psi$.

According to Newton-Euler equation, the position and attitude dynamics equations are expressed as follows:

$$m\ddot{\varsigma} = R_{\mathbb{B} \rightarrow \mathbb{E}} F_b - G_z - k_p \dot{\xi} + m d_p \quad (2)$$

$$J_b \ddot{\xi} = -(\dot{\xi} \times J_b \cdot \dot{\xi}) + T_q - k_a \dot{\xi} + J_b d_a \quad (3)$$

where m presents the mass. $G_z = [0 \ 0 \ mg]^T$. g indicates the acceleration of gravity. $F_b = [0, 0, u_f]^T$. u_f is the thrust input. $d_p = [d_x, d_y, d_z]^T$ and $d_a = [d_\phi, d_\theta, d_\psi]^T$ denote the external disturbances. $k_p = \text{diag}[k_x, k_y, k_z]$ and $k_a = \text{diag}[k_\phi, k_\theta, k_\psi]$ are the resistance coefficient matrix. $J_b = \text{diag}[J_x, J_y, J_z]$ is the inertia matrix. $T_q = [u_\phi, u_\theta, u_\psi]^T$ represents torque input. The thrust input u_f and torque input T_q can be written as:

$$\begin{bmatrix} u_f \\ u_\phi \\ u_\theta \\ u_\psi \end{bmatrix} = \begin{bmatrix} b(\varpi_1^2 + \varpi_2^2 + \varpi_3^2 + \varpi_4^2) \\ lb(\varpi_2^2 - \varpi_4^2) \\ lb(\varpi_3^2 - \varpi_1^2) \\ \nu(\varpi_2^2 + \varpi_4^2 - \varpi_3^2 - \varpi_1^2) \end{bmatrix} \quad (4)$$

where l is the length of the quadrotor arm. ϖ_i ($i = 1, \dots, 4$) denotes speed of each rotor. ν is a positive drag constant. b is a positive coefficient. Therefore, the quadrotor dynamics equation can be described as:

$$\begin{cases} \ddot{x} = \frac{1}{m}(u_f(\sin \phi \sin \psi + \sin \theta \cos \phi \cos \psi) - k_x \dot{x}) + d_x \\ \ddot{y} = \frac{1}{m}(u_f(-\cos \psi \sin \phi + \cos \phi \sin \theta \sin \psi) - k_y \dot{y}) + d_y \\ \ddot{z} = \frac{1}{m}(u_f \cos \phi \cos \theta - k_z \dot{z}) - g + d_z \\ \dot{\phi} = \frac{1}{J_x}(\dot{\theta}\dot{\psi}(J_y - J_z) + u_\phi - k_\phi \phi) + d_\phi \\ \dot{\theta} = \frac{1}{J_y}(\dot{\phi}\dot{\psi}(J_z - J_x) + u_\theta - k_\theta \theta) + d_\theta \\ \dot{\psi} = \frac{1}{J_z}(\dot{\theta}\dot{\phi}(J_x - J_y) + u_\psi - k_\psi \psi) + d_\psi \end{cases} \quad (5)$$

Consider $\chi = [x_1, x_2, \dots, x_{12}]^T = [x, \dot{x}, y, \dot{y}, z, \dot{z}, \dot{\phi}, \dot{\theta}, \dot{\psi}, \phi, \theta, \psi]^T$, $u = [u_f, u_\phi, u_\theta, u_\psi]^T$ represent the system state vector, control input, respectively. The state-space equations of a quadrotor can be written as:

$$\begin{cases} \dot{x}_1 = x_2 \\ \dot{x}_2 = (\cos x_7 \sin x_9 \cos x_{11} + \sin x_7 \sin x_{11}) \frac{u_f}{m} - f_x + d_x \\ \dot{x}_3 = x_4 \\ \dot{x}_4 = (\cos x_7 \sin x_9 \sin x_{11} - \sin x_7 \cos x_{11}) \frac{u_f}{m} - f_y + d_y \\ \dot{x}_5 = x_6 \\ \dot{x}_6 = (\cos x_7 \cos x_9) \frac{u_f}{m} - f_z - g + d_z \\ \dot{x}_7 = x_8 \\ \dot{x}_8 = b_1 x_{10} x_{12} + c_1 u_\phi - h_1 x_8 + d_\phi \\ \dot{x}_9 = x_{10} \\ \dot{x}_{10} = b_2 x_8 x_{12} + c_2 u_\theta - h_2 x_{10} + d_\theta \\ \dot{x}_{11} = x_{12} \\ \dot{x}_{12} = b_3 x_8 x_{10} + c_3 u_\psi - h_3 x_{12} + d_\psi \end{cases} \quad (6)$$

where $f_x = \frac{k_x}{m} \dot{x}$, $f_y = \frac{k_y}{m} \dot{y}$, $f_z = \frac{k_z}{m} \dot{z}$, $b_1 = \frac{J_y - J_z}{J_x}$, $b_2 = \frac{J_z - J_x}{J_y}$, $b_3 = \frac{J_x - J_y}{J_z}$, $c_1 = \frac{1}{J_x}$, $c_2 = \frac{1}{J_y}$, $c_3 = \frac{1}{J_z}$, $h_1 = \frac{k_\phi}{J_x}$, $h_2 = \frac{k_\theta}{J_y}$, $h_3 = \frac{k_\psi}{J_z}$.

Assumption 3. d_i ($i = x, y, z, \phi, \theta, \psi$) is unknown disturbances, and $|d_i| \leq \epsilon_i$, ϵ_i is a constant which presents the upper bound of disturbances.

According to the dynamics model of quadrotor, the position and attitude are coupled. In order to establish a double closed-loop control system, let:

$$\begin{cases} u_x = (\cos x_7 \sin x_9 \cos x_{11} + \sin x_7 \sin x_{11}) \frac{u_f}{m} \\ u_y = (\cos x_7 \sin x_9 \sin x_{11} - \sin x_7 \cos x_{11}) \frac{u_f}{m} \\ u_z = (\cos x_7 \cos x_9) \frac{u_f}{m} - g \end{cases} \quad (7)$$

where $[u_x \ u_y \ u_z]^T$ is the virtual control input of the position subsystem. The u_f and ideal angles (ϕ_d, θ_d) can be written as:

$$\begin{aligned} u_f &= m \sqrt{(u_z + g)^2 + u_x^2 + u_y^2} \\ \phi_d &= \arctan\left(-\frac{\cos \psi_d u_y - \sin \psi_d u_x}{u_z + g} \cos \theta_d\right) \\ \theta_d &= \arctan\left(\frac{\cos \psi_d u_x + \sin \psi_d u_y}{u_z + g}\right) \end{aligned} \quad (8)$$

Further, since the control inputs provided by the actuators are bounded, high gain controllers are unrealistic. For this reason, we constrain the control inputs and ensure that the system is stable. At this time, u_i is the bounded control input, which can be written as:

$$u_i = \text{sats}(u_i^*) \quad (i = x, y, z, \phi, \theta, \psi) \quad (9)$$

where the $\text{sats}(u_i^*)$ is defined as:

$$\text{sats}(u_i^*) = \begin{cases} u_{imax}, u_i^* > u_{imax} \\ u_i^*, |u_i^*| \leq u_{imax} \\ -u_{imax}, u_i^* < -u_{imax} \end{cases} \quad (10)$$

where $u_{imax} > 0$, u_i^* is the control input before being constrained, then we get:

$$u_i = \text{sats}(u_i^*) = u_i^* + \delta_i \quad (11)$$

Assumption 4. δ_i ($i = x, y, z, \phi, \theta, \psi$) is an unknown and bounded parameter named saturation errors, which denotes the difference between u_i and u_i^* , and its derivative satisfies: $\dot{\delta}_i \approx 0$.

The ideal paths and the ideal attitudes are expressed as $[x_d, y_d, z_d]^T$ and $[\phi_d, \theta_d, \psi_d]^T$, respectively. The tracking errors vector is defined as:

$$\begin{bmatrix} e_1 \\ e_2 \\ e_3 \\ e_4 \\ e_5 \\ e_6 \end{bmatrix} = \begin{bmatrix} x_1 - x_d \\ x_2 - \dot{x}_d \\ x_3 - y_d \\ x_4 - \dot{y}_d \\ x_5 - z_d \\ x_6 - \dot{z}_d \end{bmatrix}, \begin{bmatrix} e_7 \\ e_8 \\ e_9 \\ e_{10} \\ e_{11} \\ e_{12} \end{bmatrix} = \begin{bmatrix} x_7 - \phi_d \\ x_8 - \dot{\phi}_d \\ x_9 - \theta_d \\ x_{10} - \dot{\theta}_d \\ x_{11} - \psi_d \\ x_{12} - \dot{\psi}_d \end{bmatrix} \quad (12)$$

Controller design

In this section, we introduce a robust adaptive fuzzy nonsingular fast terminal sliding mode controller (RAFNFTSMC) for solving tracking problem of quadrotor with random uncertainty. In Fig. 2, the control frame consists of two main components: the inner-loop and the outer-loop. The inner-loop provides the fuzzy control inputs for the tracking of the attitude angles, and fuzzy approximation effectively eliminates the negative impact of unknown uncertainty in the

inner-loop. The outer loop adopts fuzzy system to estimate switching function and unknown time-varying parameters, which suppresses chattering. All control inputs are constrained by the adaptive anti-saturation method. Both inner and outer loops use nonsingular sliding surfaces to avoid singular problem. The proposed RAFNFTSMC improves the control accuracy and robustness while reducing chattering and considering actuator saturation adequately. The specific design procedure is described in the following subsections.

Fuzzy approximation principle

Fuzzy systems have universal approximation properties¹⁹, approaching $f(s)$ with $\hat{f}(s | \sigma)$. For the fuzzy system input s , we design 5 fuzzy sets (fuzzy rules). Constructing a fuzzy system uses two steps:

Step 1: For variable s , we define 5 fuzzy sets Q_s^r ($r = 1, 2, \dots, 5$).

Step 2: 5 rules are used to construct the fuzzy system $\hat{f}(s | \sigma)$, the j th fuzzy rule of a fuzzy system can be written as:

$R^{(j)}$: If s is Q_s^r then \hat{f} is P^r . where $r=1,2,\dots,5$, P^r is the fuzzy rule set for the conclusion. Then the 1th, i th and 5th fuzzy rules are denoted as follows:

$R^{(1)}$: If s is Q_s^1 then \hat{f} is P^1 .

$R^{(i)}$: If s is Q_s^i then \hat{f} is P^i .

$R^{(5)}$: If s is Q_s^5 then \hat{f} is P^5 .

By using product-inference machine, single-value fuzzifier, and average defuzzifier, the output of the fuzzy system is obtained as:

$$\hat{f}(s | \sigma) = \frac{\sum_{r=1}^5 \bar{y}_f^r (\mu_Q^r(s))}{\sum_{r=1}^5 (\mu_Q^r(s))} \quad (13)$$

where $\mu_Q^r(s)$ is the membership functions of s , \bar{y}_f^r is the center of the P^r .

Let \bar{y}_f^r is an adjustable parameter, and put it into set $\sigma \in R^{(5)}$. $\zeta(s) = [\zeta_1(s), \zeta_2(s), \dots, \zeta_r(s)]^T$ is a fuzzy basis vector, where $\zeta_r(s)$ can be presented as:

$$\zeta_r(s) = \frac{\mu_Q^r(s)}{\sum_{r=1}^5 (\mu_Q^r(s))} \quad (14)$$

Based on Eqs. (13), (14), $\hat{f}(s | \sigma)$ can be written as:

$$\hat{f}(s | \sigma) = \hat{\sigma}^T \zeta(s) \quad (15)$$

Therefore, switching functions in the position-loop and inputs in the attitude-loop can be obtained from the fuzzy system. Moreover, we set 25 fuzzy rules to approximate the unknown function of the position-loop, and the states of the subsystem is used as the fuzzy system inputs. As shown in Fig. 3, five gaussian membership functions are selected for each input of fuzzy system in this paper.

Position controllers

In this section, we describe the design process of the virtual control law u_v ($v = x, y, z$) in the position-loop. Let us describe the arctangent nonsingular terminal sliding mode surfaces of the position subsystem as follow:

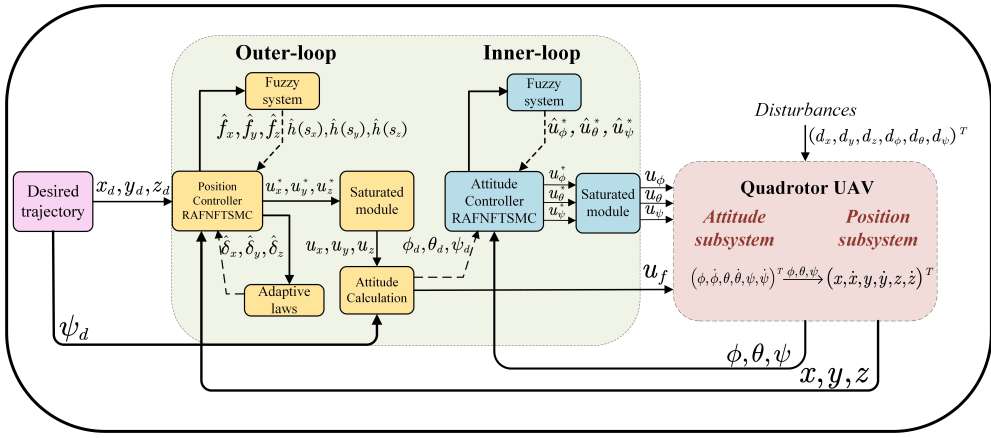


Figure 2. Control block diagram.

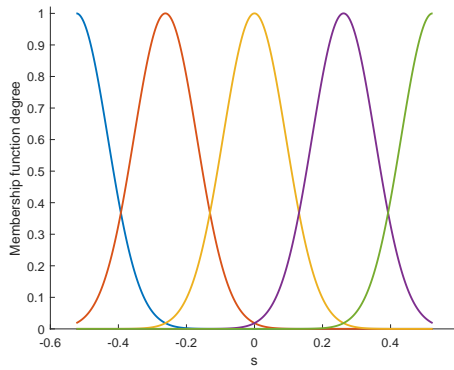


Figure 3. Membership function degree.

$$\begin{aligned}
 s_x &= e_2 + \alpha_1(1 + e_1^2)|\arctan(e_1)|^{\gamma_x} \text{sign}(\arctan(e_1)) \\
 &\quad + \beta_1 \arctan(e_1)(1 + e_1^2) \\
 s_y &= e_4 + \alpha_3(1 + e_3^2)|\arctan(e_3)|^{\gamma_y} \text{sign}(\arctan(e_3)) \\
 &\quad + \beta_3 \arctan(e_3)(1 + e_3^2) \\
 s_z &= e_6 + \alpha_5(1 + e_5^2)|\arctan(e_5)|^{\gamma_z} \text{sign}(\arctan(e_5)) \\
 &\quad + \beta_5 \arctan(e_5)(1 + e_5^2)
 \end{aligned} \tag{16}$$

where α_n, β_n ($n = 1, 3, 5$) are positive constants. $1 < \gamma_v < 2$ ($v = x, y, z$). The derivative of the sliding surfaces can be written as:

$$\begin{aligned}
 \dot{s}_x &= \dot{x}_2 - \ddot{x}_d + w_x = u_x^* + \delta_x - f_x + d_x - \ddot{x}_d + w_x \\
 \dot{s}_y &= \dot{x}_4 - \ddot{y}_d + w_y = u_y^* + \delta_y - f_y + d_y - \ddot{y}_d + w_y \\
 \dot{s}_z &= \dot{x}_6 - \ddot{y}_d + w_y = u_z^* + \delta_z - f_z + d_z - \ddot{z}_d + w_z
 \end{aligned} \tag{17}$$

where $w_v = 2\alpha_i e_i e_{i+1} |\arctan(e_i)|^{\gamma_v} \text{sign}(\arctan(e_i)) + \alpha_i \gamma_v |\arctan(e_i)|^{\gamma_v-1} e_{i+1} + 2\beta_i \arctan(e_i) e_i e_{i+1} + \beta_i e_{i+1}$, ($v = x, y, z; i = 1, 3, 5$).

By setting $\dot{s}_v = 0$ ($v = x, y, z$), the equivalent control laws are as follow:

$$\begin{aligned}
 u_{eqx}^* &= \ddot{x}_d - w_x + \hat{f}_x - \hat{\delta}_x \\
 u_{eqy}^* &= \ddot{y}_d - w_y + \hat{f}_y - \hat{\delta}_y \\
 u_{eqz}^* &= \ddot{z}_d - w_z + \hat{f}_z - \hat{\delta}_z
 \end{aligned} \tag{18}$$

where $\hat{\delta}_x, \hat{\delta}_y, \hat{\delta}_z$ are the estimated saturation errors. We approximate the f_x, f_y, f_z with the fuzzy system output $\hat{f}_x, \hat{f}_y, \hat{f}_z$. The fuzzy system output can be denoted as:

$$\hat{f}_v(\mathbf{p}_v | \hat{\sigma}_{fv}) = \hat{\sigma}_{fv}^T \zeta(\mathbf{p}_v) \quad (v = x, y, z) \tag{19}$$

where $\mathbf{p}_v = [v, \dot{v}]^T$ represents the fuzzy inputs regarding to \hat{f}_v . $\zeta(\mathbf{p}_v)$ are fuzzy basis vectors; $\hat{\sigma}_{fv}^T$ and $\hat{\delta}_v$ change based on the adaptive laws. We use the following adaptive laws:

$$\dot{\hat{\sigma}}_{fv} = -r_v s_v \zeta(\mathbf{p}_v), \quad \dot{\hat{\delta}}_v = \varphi_v \sigma_v \tag{20}$$

where $r_v, \varphi_v > 0$.

The quadrotor tracking process is subject to unknown disturbances, such as sensors noises, so we give the switching control law u_{sw} to resist the unknown disturbances²⁰. The switching control law uses a novel fast reaching law as follow:

$$u_{sw} = -\lambda |s|^m \text{sign}(s) - \mu |s|^{n \text{sign}(|s|-1)} s - \eta \text{sign}(s) \tag{21}$$

where $\lambda > 0, \mu > 0, 0 < m < 1, 0 < n < 1, \eta > |d|$.

Thus, the switching control laws of position subsystem are provided as:

$$\begin{aligned}
 u_{swv}^* &= -\lambda_v |s_v|^m \text{sign}(s_v) - \mu_v |s_v|^{n_v \text{sign}(|s_v|-1)} s_v \\
 &\quad - \eta_v \text{sign}(s_v)
 \end{aligned} \tag{22}$$

where $\lambda_v, \mu_v, m_v, n_v, \eta_v$ ($v = x, y, z$) are positive constants. When the unknown disturbances is large, the switching function gain also needs to be increased, which causes chattering. We approximate the $\eta_v \text{sign}(s_v)$ with the fuzzy system output $\hat{h}(s_v | \hat{\sigma}_{hv})$. The fuzzy system output can be denoted as:

$$\hat{h}(s_v | \hat{\sigma}_{hv}) = \hat{\sigma}_{hv}^T \zeta(s_v) \tag{23}$$

where $\zeta(s_v)$ are fuzzy basis vectors; $\hat{\sigma}_{hv}^T$ changes based on the adaptive laws. The adaptive laws is:

$$\dot{\hat{\sigma}}_{hv} = \rho_v s_v \zeta(s_v) \tag{24}$$

where $\rho_v > 0$ ($v = x, y, z$).

The virtual inputs u_x^* , u_y^* , and u_z^* can be presented as:

$$\left\{ \begin{array}{l} u_x^* = u_{eqx}^* + u_{swx}^* \\ \quad = \ddot{x}_d - w_x + \hat{f}_x - \hat{\delta}_x - \lambda_x |s_x|^{m_x} \text{sign}(s_x) - \mu_x \\ \quad \quad |s_x|^{n_x \text{sign}(|s_x|-1)} s_x - \hat{h}(s_x | \hat{\sigma}_{hx}) \\ u_y^* = u_{eqy}^* + u_{swy}^* \\ \quad = \ddot{y}_d - w_y + \hat{f}_y - \hat{\delta}_y - \lambda_y |s_y|^{m_y} \text{sign}(s_y) - \mu_y \\ \quad \quad |s_y|^{n_y \text{sign}(|s_y|-1)} s_y - \hat{h}(s_y | \hat{\sigma}_{hy}) \\ u_z^* = u_{eqz}^* + u_{swz}^* \\ \quad = \ddot{z}_d - w_z + \hat{f}_z - \hat{\delta}_z - \lambda_z |s_z|^{m_z} \text{sign}(s_z) - \mu_z \\ \quad \quad |s_z|^{n_z \text{sign}(|s_z|-1)} s_z - \hat{h}(s_z | \hat{\sigma}_{hz}) \end{array} \right. \quad (25)$$

Lemma 1. ²¹ Consider a system that satisfies the following inequality:

$$\dot{V}(x) + kV^\Upsilon(x) \leq 0 \quad (26)$$

where $0 < \Upsilon < 1$, $k > 0$, $V(x)$ denotes a positive Lyapunov function, $x \in R$ represents the state of system. System converges to origin in the finite time. The convergence time from $V(x(0))$ to zero can be calculated as:

$$t_a \leq \frac{V^{1-\Upsilon}(x(0))}{k(1-\Upsilon)} \quad (27)$$

Theorem 1. Considering the x-subsystem (5) with the surface (16). The controllers and the adaptive laws are designed as (25) and (20), (24). The x-system converges asymptotically to $s_x = 0$, then the error e_1 converges to zero in a finite time. For y-system and z-system, the above results also holds.

Proof. Define optimal parameters:

$$\hat{\sigma}_{fx}^* = \arg \min_{\hat{\sigma}_{fx} \in \Omega_{fx}} [\sup |\hat{f}_x(\mathbf{p}_x | \hat{\sigma}_{fx}) - f_x|] \quad (28)$$

$$\hat{\sigma}_{hx}^* = \arg \min_{\hat{\sigma}_{hx} \in \Omega_{hx}} [\sup |\hat{h}(s_x | \hat{\sigma}_{hx}) - \eta_x \text{sign}(s_x)|] \quad (29)$$

where Ω_{fx} is the set of $\hat{\sigma}_{fx}$, and $f_x = \hat{f}(\mathbf{p}_x | \hat{\sigma}_{fx}^*)$. Ω_{hx} is the set of $\hat{\sigma}_{hx}$, and $\eta_x \text{sign}(s_x) = \hat{h}(s_x | \hat{\sigma}_x^*)$.

Then we define a Lyapunov function as follows:

$$V_x = \frac{1}{2}s_x^2 + \frac{1}{2\rho_x} \tilde{\sigma}_{hx}^T \tilde{\sigma}_{hx} + \frac{1}{2r_x} \tilde{\sigma}_{fx}^T \tilde{\sigma}_{fx} + \frac{1}{2\varphi_x} \tilde{\delta}_x^2 \quad (30)$$

where $\tilde{\sigma}_{hx} = \hat{\sigma}_{hx}^* - \hat{\sigma}_{hx}$, $\dot{\tilde{\sigma}}_{hx} = -\dot{\hat{\sigma}}_{hx}$, $\rho_x > 0$. $\tilde{\sigma}_{fx} = \hat{\sigma}_{fx}^* - \hat{\sigma}_{fx}$, $\dot{\tilde{\sigma}}_{fx} = -\dot{\hat{\sigma}}_{fx}$, $r_x > 0$. $\tilde{\delta}_x = \hat{\delta}_x - \delta_x$, $\varphi_x > 0$.

The derivative of V_x can be written as:

$$\begin{aligned} \dot{V}_x &= s_x \dot{s}_x - \frac{1}{\rho_x} \tilde{\sigma}_{hx}^T \dot{\tilde{\sigma}}_{hx} - \frac{1}{r_x} \tilde{\sigma}_{fx}^T \dot{\tilde{\sigma}}_{fx} + \frac{1}{\varphi_x} \tilde{\delta}_x \dot{\tilde{\delta}}_x \\ &= s_x(u_x^* + \delta_x - f_x + d_x - \ddot{x}_d + w_x) - \frac{1}{\rho_x} \tilde{\sigma}_{hx}^T \dot{\tilde{\sigma}}_{hx} \\ &\quad - \frac{1}{r_x} \tilde{\sigma}_{fx}^T \dot{\tilde{\sigma}}_{fx} + \frac{1}{\varphi_x} \tilde{\delta}_x \dot{\tilde{\delta}}_x \\ &= s_x(\hat{f}_x - f_x - \tilde{\delta}_x + d_x - \lambda_x |s_x|^{m_x} \text{sign}(s_x) \\ &\quad - \mu_x |s_x|^{n_x \text{sign}(|s_x|-1)} s_x - \hat{h}(s_x | \hat{\sigma}_{hx})) - \frac{1}{\rho_x} \tilde{\sigma}_{hx}^T \dot{\tilde{\sigma}}_{hx} \\ &\quad - \frac{1}{r_x} \tilde{\sigma}_{fx}^T \dot{\tilde{\sigma}}_{fx} + \frac{1}{\varphi_x} \tilde{\delta}_x \dot{\tilde{\delta}}_x \end{aligned}$$

$$\begin{aligned} &= s_x(-\tilde{\sigma}_{fx}^T \zeta(\mathbf{p}_x) - \tilde{\delta}_x + d_x - \lambda_x |s_x|^{m_x} \text{sign}(s_x) \\ &\quad - \mu_x |s_x|^{n_x \text{sign}(|s_x|-1)} s_x + \tilde{\sigma}_{hx}^T \zeta(s_x) - \hat{h}(s_x | \hat{\sigma}_{hx}^*)) \\ &\quad - \frac{1}{\rho_x} \tilde{\sigma}_{hx}^T \dot{\tilde{\sigma}}_{hx} - \frac{1}{r_x} \tilde{\sigma}_{fx}^T \dot{\tilde{\sigma}}_{fx} + \frac{1}{\varphi_x} \tilde{\delta}_x \dot{\tilde{\delta}}_x \\ &= s_x(d_x - \lambda_x |s_x|^{m_x} \text{sign}(s_x) - \mu_x |s_x|^{n_x \text{sign}(|s_x|-1)} s_x \\ &\quad - \eta_x \text{sign}(s_x)) + \tilde{\delta}_x \left(\frac{\dot{\tilde{\delta}}_x}{\varphi_x} - s_x \right) \\ &\quad + \tilde{\sigma}_{hx}^T(s_x \zeta(s_x) - \frac{1}{\rho_x} \dot{\tilde{\sigma}}_{hx}) - \tilde{\sigma}_{fx}^T(s_x \zeta(\mathbf{p}_x) + \frac{1}{r_x} \dot{\tilde{\sigma}}_{fx}) \end{aligned} \quad (31)$$

Substituting the Eqs. (20), (24) into Eq. (31), then we get:

$$\begin{aligned} \dot{V}_x &= s_x(d_x - \lambda_x |s_x|^{m_x} \text{sign}(s_x) - \mu_x |s_x|^{n_x \text{sign}(|s_x|-1)} s_x \\ &\quad - \eta_x \text{sign}(s_x)) \\ &\leq |s_x| |d_x| - \lambda_x |s_x|^{m_x+1} - \mu_x |s_x|^{n_x \text{sign}(|s_x|-1)+2} - \eta_x |s_x| \\ &\leq -(\eta_x |s_x| - |s_x| \epsilon_x + \lambda_x |s_x|^{m_x+1} + \mu_x |s_x|^{n_x \text{sign}(|s_x|-1)+2}) \\ &\leq 0 \end{aligned} \quad (32)$$

while $\dot{V}_x \equiv 0$, $s_x \equiv 0$, according to LaSalle's invariant set principle, $t \rightarrow \infty$, $s_x \rightarrow 0$. The x-system asymptotic stability is ensured. The y-system, z-system are asymptotically stable by using similar proof methods and the process is omitted here.

Furthermore, when the system is on $s_x = 0$, for the system $\dot{e}_1 = -\alpha_1(1+e_1^2)|\arctan(e_1)|^{\gamma_x} \text{sign}(\arctan(e_1)) - \beta_1 \arctan(e_1)(1+e_1^2)$. let $\vartheta = \arctan(e_1)$, $\vartheta \rightarrow 0$, $e_1 \rightarrow 0$. Defining the Lyapunov function $V_\vartheta = \frac{1}{2}\vartheta^2$, we have:

$$\begin{aligned} \dot{V}_\vartheta &= \vartheta \dot{\vartheta} = \vartheta \frac{\dot{e}_1}{1+e_1^2} \\ &= \vartheta(-\alpha_1|\arctan(e_1)|^{\gamma_x} \text{sign}(\arctan(e_1)) - \beta_1 \arctan(e_1)) \\ &= \vartheta(-\alpha_1|\vartheta|^{\gamma_x} \text{sign}(\vartheta) - \beta_1 \vartheta) \\ &= -\alpha_1|\vartheta|^{\gamma_x+1} - \beta_1 \vartheta^2 \\ &\leq -(\alpha_1|\vartheta|^{\gamma_x} + \beta_1|\vartheta|)\sqrt{2} \frac{|\vartheta|}{\sqrt{2}} \\ &\leq -\sqrt{2}k V_\vartheta^{\frac{1}{2}}(t) \end{aligned} \quad (33)$$

where $k = \alpha_1|\vartheta|^{\gamma_x} + \beta_1|\vartheta|$. According to the Lemma 1, e_1 converges to zero in finite time which is:

$$t_p \leq \frac{\sqrt{2V_\vartheta(0)}}{k} \quad (34)$$

This completes the proof.

Attitude controllers

The goal of this section is to design adaptive inputs fuzzy integral sliding mode controllers that forces the error signal e_j ($j = 7, 9, 11$) of attitude loop to converge to zero in finite time. A fast terminal integral sliding surface is adopted for attitude subsystem¹⁵, which is as follows:

$$\begin{aligned} s_\phi &= e_8 + \int_0^t \alpha_7 |e_7|^{\ell_{\phi 1}} \text{sign}(e_7) + \beta_7 |e_8|^{\ell_{\phi 2}} \text{sign}(e_8) dt \\ s_\theta &= e_{10} + \int_0^t \alpha_9 |e_9|^{\ell_{\theta 1}} \text{sign}(e_9) + \beta_9 |e_{10}|^{\ell_{\theta 2}} \text{sign}(e_{10}) dt \end{aligned}$$

$$s_\psi = e_{12} + \int_0^t \alpha_{11}|e_{11}|^{\ell_{\psi 1}} \text{sign}(e_{11}) + \beta_{11}|e_{12}|^{\ell_{\psi 2}} \text{sign}(e_{12}) dt \quad (35)$$

where α_j, β_j ($j = 7, 9, 11$) are the positive parameters, ℓ_{i1}, ℓ_{i2} ($i = \phi, \theta, \psi$) must be selected to meet:

$$\begin{cases} \ell_{i1} \in (0, 1) \\ \ell_{i2} = \frac{2\ell_{i1}}{1+\ell_{i1}} \end{cases} \quad (36)$$

The derivative of the sliding mode surfaces are offered as follows:

$$\begin{cases} \dot{s}_\phi = b_1 x_{10} x_{12} + c_1(u_\phi^* + \delta_\phi) - h_1 x_8 + d_\phi - \ddot{\phi}_d \\ \quad + \alpha_7 |e_7|^{\ell_{\phi 1}} \text{sign}(e_7) + \beta_7 |e_8|^{\ell_{\phi 2}} \text{sign}(e_8) \\ \dot{s}_\theta = b_2 x_8 x_{12} + c_2(u_\theta^* + \delta_\theta) - h_2 x_{10} + d_\theta - \ddot{\theta}_d \\ \quad + \alpha_9 |e_9|^{\ell_{\theta 1}} \text{sign}(e_9) + \beta_9 |e_{10}|^{\ell_{\theta 2}} \text{sign}(e_{10}) \\ \dot{s}_\psi = b_3 x_8 x_{10} + c_3(u_\psi^* + \delta_\psi) - h_3 x_{12} + d_\psi - \ddot{\psi}_d \\ \quad + \alpha_{11} |e_{11}|^{\ell_{\psi 1}} \text{sign}(e_{11}) + \beta_{11} |e_{12}|^{\ell_{\psi 2}} \text{sign}(e_{12}) \end{cases} \quad (37)$$

when the sliding mode control is in the ideal state $s(t) = \dot{s}(t) = 0$, the tracking error will converge to zero. Assuming that any uncertainty are known, the ideal control laws can be obtained based on Eq. (37):

$$\begin{cases} \bar{u}_\phi^*(t) = \frac{1}{c_1}(-b_1 x_{10} x_{12} + h_1 x_8 - d_\phi + \ddot{\phi}_d \\ \quad - \alpha_7 |e_7|^{\ell_{\phi 1}} \text{sign}(e_7) - \beta_7 |e_8|^{\ell_{\phi 2}} \text{sign}(e_8)) - \delta_\phi \\ \bar{u}_\theta^*(t) = \frac{1}{c_2}(-b_2 x_8 x_{12} + h_2 x_{10} - d_\theta + \ddot{\theta}_d \\ \quad - \alpha_9 |e_9|^{\ell_{\theta 1}} \text{sign}(e_9) - \beta_9 |e_{10}|^{\ell_{\theta 2}} \text{sign}(e_{10})) - \delta_\theta \\ \bar{u}_\psi^*(t) = \frac{1}{c_3}(-b_3 x_8 x_{10} + h_3 x_{12} - d_\psi + \ddot{\psi}_d \\ \quad - \alpha_{11} |e_{11}|^{\ell_{\psi 1}} \text{sign}(e_{11}) - \beta_{11} |e_{12}|^{\ell_{\psi 2}} \text{sign}(e_{12})) - \delta_\psi \end{cases} \quad (38)$$

According to fuzzy approximation theory, there exists an optimal fuzzy system $u_{fz}(s, \sigma^*)$ approximating $\bar{u}^*(t)$.

$$\bar{u}^*(t) = u_{fz}(s, \sigma^*) + \varepsilon = \sigma^{*T} \zeta(s) + \varepsilon \quad (39)$$

where ε is an approximation error, $|\varepsilon| < E$.

Using the fuzzy system $u_{fz}(s, \hat{\sigma})$ to approximate $u^*(t)$, we can get:

$$u_{fz}(s, \hat{\sigma}) = \hat{\sigma}^T \zeta(s) \quad (40)$$

where $\hat{\sigma}$ is the estimated value of σ^* .

u_{vs} is used to compensate for the error between \bar{u}^* and u_{fz} , and the controllers can be expressed as:

$$\begin{cases} u_\phi^* = u_{fz\phi} + u_{vs\phi} = \hat{\sigma}_\phi^T \zeta(s_\phi) - \hat{E}_\phi \text{sign}(s_\phi) \\ u_\theta^* = u_{fz\theta} + u_{vs\theta} = \hat{\sigma}_\theta^T \zeta(s_\theta) - \hat{E}_\theta \text{sign}(s_\theta) \\ u_\psi^* = u_{fz\psi} + u_{vs\psi} = \hat{\sigma}_\psi^T \zeta(s_\psi) - \hat{E}_\psi \text{sign}(s_\psi) \end{cases} \quad (41)$$

where $\hat{\sigma}_i^T, \hat{E}_i$ ($i = \phi, \theta, \psi$) change based on the adaptive laws.

The expression of the adaptive laws are:

$$\dot{\hat{\sigma}}_i = -\rho_i s_i \zeta(s_i), \quad \dot{\hat{E}}_i = \eta_i |s_i| \quad (42)$$

where $\rho_i, \eta_i > 0$ ($i = \phi, \theta, \psi$).

Theorem 2. Considering the ϕ -subsystem (5) with the surface (35). The controllers and the adaptive laws are designed as (41), (42). The ϕ -system converges asymptotically to $s_\phi = 0$, then the error e_7 converges to zero in a finite time. For θ -system and ψ -system, the above results also holds.

Proof. Based on Eqs. (39), (40), we can get:

$$\tilde{u}_{fz\phi} = \hat{u}_{fz\phi} - \bar{u}_\phi^* = \hat{u}_{fz\phi} - u_{fz\phi}^* - \varepsilon \quad (43)$$

then we define $\tilde{\sigma}_\phi = \hat{\sigma}_\phi - \sigma_\phi^*$, Eq. (43) becomes:

$$\tilde{u}_{fz\phi} = \tilde{\sigma}_\phi^T \zeta(s_\phi) - \varepsilon \quad (44)$$

Based on Eq. (35), we can get:

$$\dot{s}_\phi = \dot{x}_8 - \ddot{\phi}_d + \alpha_7 |e_7|^{\ell_{\phi 1}} \text{sign}(e_7) + \beta_7 |e_8|^{\ell_{\phi 2}} \text{sign}(e_8) \quad (45)$$

The Eq. (38) can be written as:

$$\begin{aligned} \bar{u}_\phi^* &= \frac{1}{c_1}(-b_1 x_{10} x_{12} + h_1 x_8 - d_\phi + \dot{x}_8 - \dot{s}_\phi - c_1 \delta_\phi) \\ &= \frac{1}{c_1}(c_1 u_\phi^* - \dot{s}_\phi) \end{aligned} \quad (46)$$

From Eqs. (41), (46), we have:

$$\dot{s}_\phi = c_1(u_\phi^* - \bar{u}_\phi^*) = c_1(u_{fz\phi} + u_{vs\phi} - \bar{u}_\phi^*) \quad (47)$$

Define a Lyapunov function:

$$V_\phi = \frac{1}{2}\sigma_\phi^2 + \frac{c_1}{2\rho_\phi^*} \tilde{\varphi}_\phi^T \tilde{\varphi}_\phi + \frac{c_1}{2r_\phi^*} \tilde{E}_\phi^2 \quad (48)$$

where $\tilde{E}_\phi = \hat{E}_\phi - E_\phi$, $c_1 > 0$, the derivative of V_ϕ can be written as:

$$\begin{aligned} \dot{V}_\phi &= s_\phi \dot{s}_\phi + \frac{c_1}{\rho_\phi} \tilde{\sigma}_\phi^T \dot{\tilde{\sigma}}_\phi + \frac{c_1}{\eta_\phi} \tilde{E}_\phi \dot{\tilde{E}}_\phi \\ &= s_\phi c_1(u_{fz\phi} + u_{vs\phi} - \bar{u}_\phi^*) + \frac{c_1}{\rho_\phi} \tilde{\sigma}_\phi^T \dot{\tilde{\sigma}}_\phi + \frac{c_1}{\eta_\phi} \tilde{E}_\phi \dot{\tilde{E}}_\phi \\ &= s_\phi c_1(\tilde{u}_{fz\phi} + u_{vs\phi}) + \frac{c_1}{\rho_\phi} \tilde{\sigma}_\phi^T \dot{\tilde{\sigma}}_\phi + \frac{c_1}{\eta_\phi} \tilde{E}_\phi \dot{\tilde{E}}_\phi \\ &= s_\phi c_1(\tilde{\sigma}_\phi^T \zeta(s_\phi) - \varepsilon + u_{vs\phi}) + \frac{c_1}{\rho_\phi} \tilde{\sigma}_\phi^T \dot{\tilde{\sigma}}_\phi + \frac{c_1}{\eta_\phi} \tilde{E}_\phi \dot{\tilde{E}}_\phi \\ &= c_1 \tilde{\sigma}_\phi^T (s_\phi \zeta(s_\phi) + \frac{1}{\rho_\phi} \dot{\tilde{\sigma}}_\phi) + s_\phi c_1(u_{vs\phi} - \varepsilon) + \frac{c_1}{\eta_\phi} \tilde{E}_\phi \dot{\tilde{E}}_\phi \end{aligned} \quad (49)$$

Substituting Eqs. (41), (42) into Eq. (49), we can obtain:

$$\begin{aligned} \dot{V}_\phi &= c_1 \tilde{\sigma}_\phi^T (s_\phi \zeta(s_\phi) + \frac{1}{\rho_\phi} \dot{\tilde{\sigma}}_\phi) + s_\phi c_1(u_{vs\phi} - \varepsilon) + \frac{c_1}{\eta_\phi} \tilde{E}_\phi \dot{\tilde{E}}_\phi \\ &= -c_1 |s_\phi| \hat{E}_\phi - c_1 s_\phi \varepsilon + \frac{c_1}{\eta_\phi} (\hat{E}_\phi - E_\phi) \dot{\tilde{E}}_\phi \\ &= -c_1 |s_\phi| \hat{E}_\phi - c_1 s_\phi \varepsilon + c_1 |s_\phi| (\hat{E}_\phi - E_\phi) \\ &= -c_1 s_\phi \varepsilon - c_1 |s_\phi| E_\phi \\ &\leq c_1 |s_\phi| |\varepsilon| - c_1 |s_\phi| E_\phi \\ &\leq -(E_\phi - |\varepsilon|) c_1 |s_\phi| \\ &\leq 0 \end{aligned} \quad (50)$$

while $\dot{V}_\phi \equiv 0, s_\phi \equiv 0$, according to LaSalle's invariant set principle, $t \rightarrow \infty, s_\phi \rightarrow 0$. The ϕ -system asymptotic stability is ensured.

Further, the tracking error e_7 converges to zero in a finite time when $s_\phi = \dot{s}_\phi = 0$. Eq. (45) can be written as:

$$\begin{aligned}\dot{e}_7 &= e_8 \\ \dot{e}_8 &= -\alpha_7|e_7|^{\ell_{\phi 1}} \text{sign}(e_7) - \beta_7|e_8|^{\ell_{\phi 2}} \text{sign}(e_8)\end{aligned}\quad (51)$$

define the Lyapunov function as:

$$V_{\phi 1} = \frac{\alpha_7}{1 + \ell_{\phi 1}} |e_7|^{1+\ell_{\phi 1}} + \frac{1}{2} |e_8|^2 \quad (52)$$

then the derivative of $V_{\phi 1}$ can be gotten as:

$$\dot{V}_{\phi 1} = -\beta_7|e_8|^{1+\ell_{\phi 2}} \leq 0 \quad (53)$$

it shows that (51) is asymptotically stable after reaching $s_\phi = 0$.

There is a time t_r enables $\dot{e}_7(t_r) = 0$ and \dot{s}_ϕ can be rewritten as:

$$\alpha_7|e_7|^{\ell_{\phi 1}} \text{sign}(e_7) + \beta_7|e_8|^{\ell_{\phi 2}} \text{sign}(e_8) = 0 \quad (54)$$

we conclude that the finite convergence time for e_7 from Eq. (54):

$$\begin{aligned}t_z &= \int_0^{|e_7(0)|} \left(\frac{\beta_7}{\alpha_7} \right)^{\frac{\alpha_7+1}{2\alpha_7}} \left(e_7^{\frac{-1}{\alpha_7}} \right)^{\frac{\alpha_7+1}{2\alpha_7}} de_7 \\ &= \frac{2}{1-\alpha_7} \left(\frac{\beta_7}{\alpha_7} \right)^{\frac{\alpha_7+1}{2\alpha_7}} |e_7(0)|^{\frac{1-\alpha_7}{2}}\end{aligned}\quad (55)$$

The θ -system, ψ -system are asymptotically stable by using similar proof methods and the process is omitted here. All proofs are completed.

Simulation results

In this section, we verify the effectiveness of the proposed RAFNFTSMC method in simulation. To highlight the advantages of the proposed RAFNFTSMC method, we make a comparison with NTSMC, FGNTSMC^{4,18}. Consider the physical parameters of the quadrotor used in simulation as: $m = 0.486$ Kg, $l = 0.25$ m, $g = 9.8$ m/s², $J_x = 3.8278e-3$ Kg·m², $J_y = 3.8278e-3$ Kg·m², $J_z = 7.6566e-3$ Kg·m², $k_x = k_y = k_z = 5.5670e-4$ N·s/m, $k_\phi = k_\theta = k_\psi = 5.5670e-4$ N·s/rad.

Consider the parameters of the controller as: $\alpha_1 = \alpha_3 = 1.2$, $\alpha_5 = 10$, $\beta_1 = \beta_3 = 1.2$, $\beta_5 = 10$, $\gamma_x = \gamma_y = \gamma_z = 1.001$, $\lambda_x = \lambda_y = \lambda_z = 4.5$, $\mu_z = 1.5$, $\mu_x = \mu_y = 1.0$, $\rho_x = \rho_y = 5.85$, $\rho_z = 10$, $m_x = m_y = 0.52$, $m_z = 0.3$, $n_x = n_y = n_z = 0.3$, $\rho_\phi = \rho_\theta = \rho_\psi = 10$, $\alpha_7 = \alpha_9 = 25$, $\alpha_{11} = 8$, $\beta_7 = \beta_9 = 19$, $\beta_{11} = 5.5$, $\eta_\phi = \eta_\theta = \eta_\psi = 1$.

Instead of choosing a fixed constant for $\ell_{i1}(i = \phi, \theta, \psi)$, we use an empirical function as follows:

$$\ell_{i1} = \exp[-(|e_j| + 0.23)^{1.1} - (|e_j| + 0.21)^{0.71}] + 0.4 \quad (56)$$

where $j = 7, 9, 11$. It is a monotonically decreasing function with error as the independent variable, which weakens the chattering when the error is small.

The parameters of the quadrotor are selected from <https://www.flyeval.com/>. The control input is allocated according to the maximum thrust and channels

priority. Torque input is similar to duty cycle from -1 to 1 . Based on the control allocation of each channel, we set the following constraints for the inputs in this paper:

$$\begin{aligned}|u_x| &\leq 2 \text{ N}, |u_y| \leq 2 \text{ N}, |u_z| \leq 7 \text{ N} \\ |u_\phi| &\leq 1 \text{ N} \cdot \text{m}, |u_\theta| \leq 1 \text{ N} \cdot \text{m}, |u_\psi| \leq 1 \text{ N} \cdot \text{m}\end{aligned}\quad (57)$$

We give two cases for validating the robustness and efficiency of the proposed RAFNFTSMC method. In all cases, random uncertainty and unknown disturbances is fully considered. For time-varying mass, we provide mass loss such as parts falling off for case 1 and mass loss with loading for case 2. This effect is showed in Fig. 4a. Moreover, the 30% random variation in resistance coefficient and the moment of inertia are considered, which are presented in Fig. 4b. To further confirm the superiority of the proposed RAFNFTSMC, random noises are also taken into account in case 2. This performance is displayed in Fig. 4c.

Case 1

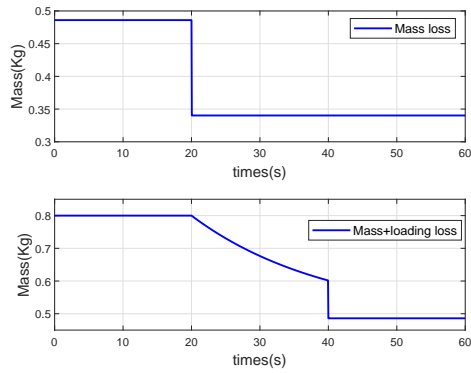
In this case, we provide a 3-D desired trajectory for quadrotor as follows:

$$\begin{aligned}x_d &= \begin{cases} 2 \text{ m}, t \in [0, 2\pi] \\ \sin(t) + 2 \text{ m}, t \in (2\pi, 50] \end{cases} \\ y_d &= \begin{cases} 2 \text{ m}, t \in [0, 2\pi] \\ \cos(t) + 1 \text{ m}, t \in (2\pi, 50] \end{cases} \\ z_d &= \begin{cases} 2 \text{ m}, t \in [0, 2\pi] \\ 1 + \cos^2(t) + 2 \sin^2(t) \text{ m}, t \in (2\pi, 50] \end{cases} \\ \psi_d &= 3.75^\circ, t \in [0, 50]\end{aligned}\quad (58)$$

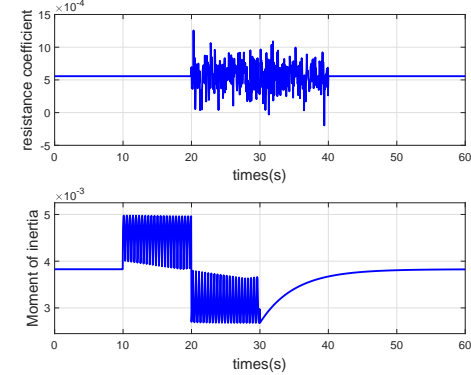
The unknown disturbances are selected as follows:

$$\begin{aligned}d_x &= 0.3 \sin\left(\frac{\pi t}{3}\right) \text{ m/s}^2, d_\phi = \cos\left(\frac{\pi t}{5}\right) \text{ rad/s}^2, \\ d_y &= 0.3 \sin\left(\frac{\pi t}{3}\right) \text{ m/s}^2, d_\theta = \sin(0.7t) \text{ rad/s}^2, \\ d_z &= 1.2 \sin(t) \text{ m/s}^2, d_\psi = \cos(t) \text{ rad/s}^2\end{aligned}\quad (59)$$

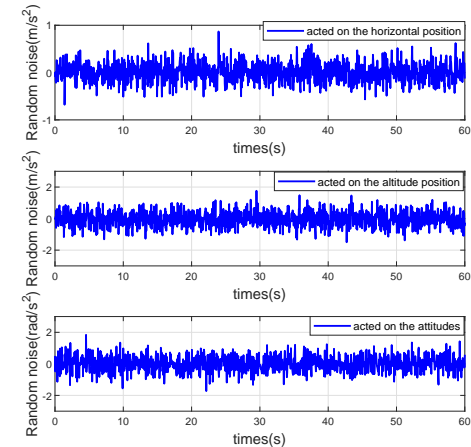
Fig. 5a shows the effect of the 3-D flight path accompanied by the FGNTSMC, NTSMC, the proposed RAFNFTSMC controllers. Figs. 6a-6b illustrate the performance of position and attitude tracking. It can be observed that the position/attitude can track accurately under mass loss and unknown disturbances. In Fig. 7a, the controller signals is smooth except when the trajectory changes abruptly. When the trajectory changes abruptly, the control signal does not show very drastic changes. Fig. 7b shows that the proposed method has an outstanding anti-chattering effect than the other methods. The adaptive gains of the attitude loop for compensating the fuzzy approximation errors is given in Fig. 5b.



(a) Mass loss.



(b) Random parameters.



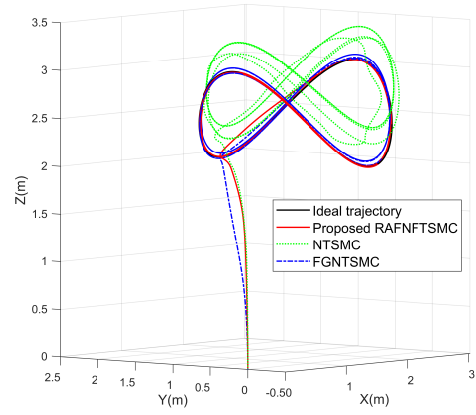
(c) Random noises.

Figure 4. Random uncertainty.

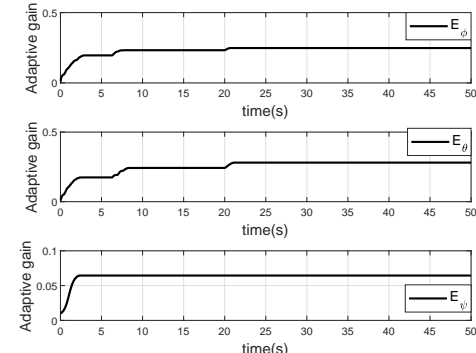
Case 2

In this case, the desired trajectory is defined as follow:

$$\begin{aligned} x_d &= \begin{cases} 0 \text{ m}, & t \in [0, 7] \\ 2 \text{ m}, & t \in (7, 15] \\ 1 + \cos(t - 15) \text{ m}, & t \in (15, 60] \end{cases} \\ y_d &= \begin{cases} 0 \text{ m}, & t \in [0, 7] \\ 2 \text{ m}, & t \in (7, 15] \\ 2 - \sin(t - 15) \text{ m}, & t \in (15, 60] \end{cases} \\ z_d &= \begin{cases} \frac{2t}{7} \text{ m}, & t \in [0, 7] \\ 2 \text{ m}, & t \in (7, 15] \\ 1 + e^{-0.3(t-15)} \text{ m}, & t \in (15, 60] \end{cases} \\ \psi_d &= 3.75^\circ, \quad t \in [0, 60] \end{aligned} \quad (60)$$



(a) 3-D tracking.



(b) Adaptive gains in case 1.

Figure 5. Tracking and adaptive gains in case 1.

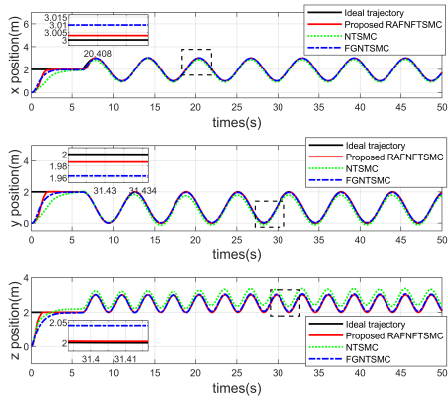
The 3-D tracking results are shown in Fig. 8a, which contains the effects of the compared methods. The adaptive gains variation process of the attitude loop is shown in Fig. 8b. In Fig. 9a- 9b, it can be viewed that the proposed RAFNFTSMC keeps precise tracking and high robustness against random noises and loading loss. Fig. 10a displays that the control signal changes slightly firstly and then stably remains near zero. In Fig. 10b, the chattering condition of the compared methods is worse. Finally, two set of comparison tests for performance indexes is applied to evaluate the distinction between the proposed RAFNFTSMC, NTSMC, FGNTSMC^{4,18}. The error squared integration (ESI) can be described as follows:

$$\text{ESI} = \int_{t_0}^{t_s} e^2 dt \quad (61)$$

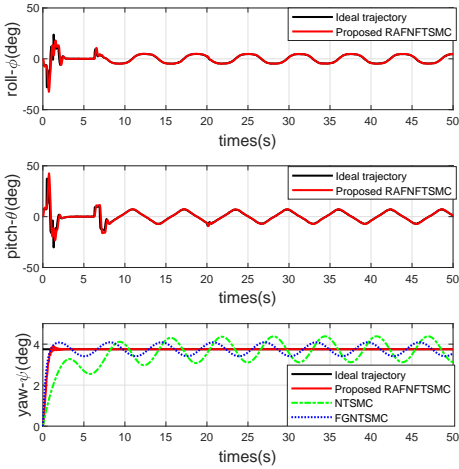
where t_0 is the initial time of the simulation, t_s presents final time, e is track error.

Remark 1. Different controllers are affected differently by the initial transient. We compare the ESI in the steady-state tracking period for a fair comparison. The initial transient time is chosen to be 2 seconds. In particular, the trajectory changes of all cases are piecewise. It is meaningful to exclude the initial transient at each stage. In the tables 1 and 2 respecting to performance indexes, the best results are shown in bold text.

It is shown in Table 1 that the proposed idea guarantees a high accuracy and robustness compared with other methods.



(a) Position tracking.



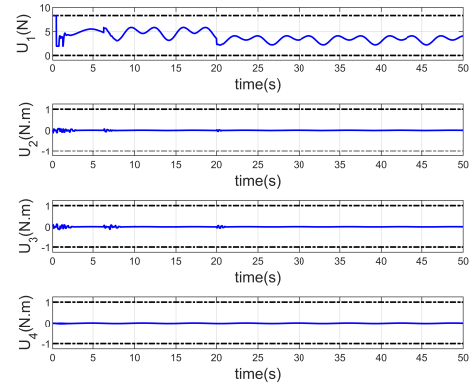
(b) Attitude tracking.

Figure 6. Tracking performance in case 1.

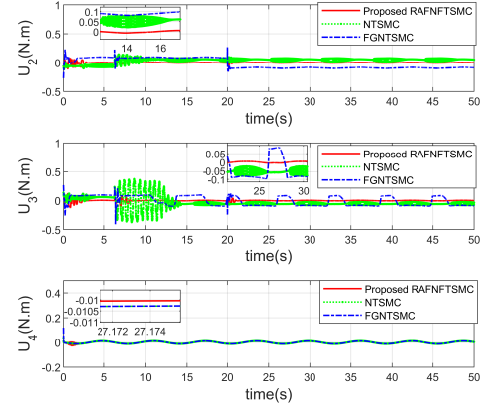
Table 1. ESI indexes

State	Proposed RAFN- FTSMC	NTSMC	FGNTSMC
case 1			
x	0.0549	1.0255	0.076
y	0.0109	1.5288	0.0621
z	0.0007	4.8853	0.1063
ϕ	0.0008	0.4441	0.0142
θ	0.0213	1.295	0.0148
ψ	0.0001	0.0038	0.0008
case 2			
x	0.0066	1.0471	0.2926
y	0.0283	1.1331	0.0920
z	0.00018	5.0581	1.1050
ϕ	0.03	0.1623	0.122
θ	0.0141	0.3091	0.0210
ψ	0.0001	0.07	0.0023

The proposed method generally outperforms other similar methods under random uncertainty and trajectories with abnormal changes. Especially z-position tracking effect is significantly better in the face of mass loss. It is worth noting



(a) Control inputs.



(b) Control inputs comparison.

Figure 7. Control inputs in case 1.

that the other methods do not consider actuator saturation. This indicates that the results of the proposed method is meaningful. On the other hand, the IAU and the IADU are used to evaluate the controller signals, they can be described as:

$$\text{IAU} = \int_{t_0}^{t_s} |u(t)| dt, \quad \text{IADU} = \int_{t_0}^{t_s} \left| \frac{du(t)}{dt} \right| dt \quad (62)$$

where t_0 is the initial time of the simulation, t_s presents final time, $u(t)$ is the control input.

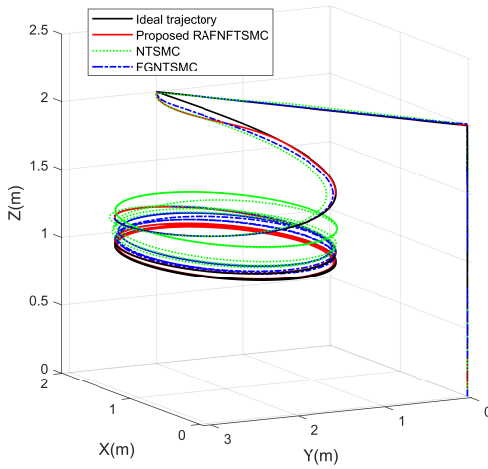
The IAU is a standard for describing the magnitude of the signal amplitude. The purpose of the IADU is to detect the smoothness of the signals. The IADU becomes more smaller, the anti-chattering ability of signals becomes more stronger. In Table 2, Both IAU and IADU values of the proposed method are smaller than those of similar methods. This indicates that the proposed method has an excellent anti-chattering capability. Lastly, the signal amplitude is tiny without excessive energy consumption. This means that the adaptive anti-saturation technique ensures that the control gain is limited to a small range.

Conclusion

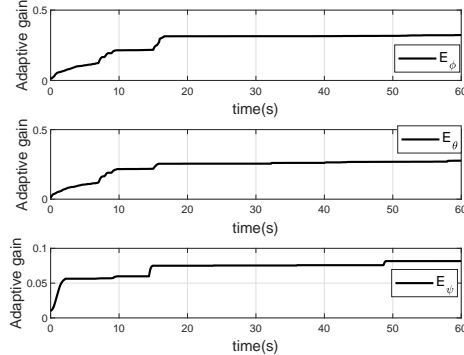
This paper proposes a novel robust adaptive fuzzy nonsingular fast terminal sliding mode controller (RAFNFTSMC) for tracking of quadrotor under uncertain factors. Adopting

Table 2. IAU and IADU performance indexes

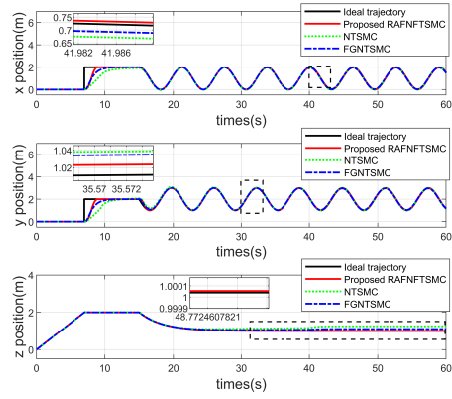
Control plan	Performance indexes					
	IAU			IADU		
	u_2	u_3	u_4	u_2	u_3	u_4
case 1						
Proposed RAFNFTSMC	0.3320	0.3726	0.3710	3.3719	3.9997	0.4129
NTSMC	6.7860	7.1785	0.5679	1.1094e+03	1.1396e+03	0.9462
FGNTSMC	6.1217	5.6028	0.3730	900.7672	816.70	0.502
case 2						
Proposed RAFNFTSMC	0.2436	0.2207	0.0469	28.5603	23.5228	3.5046
NTSMC	0.8215	0.7901	0.0803	216.6968	216.1657	25.0221
FGNTSMC	0.7163	0.6917	0.0545	91.65	91.510	4.9536



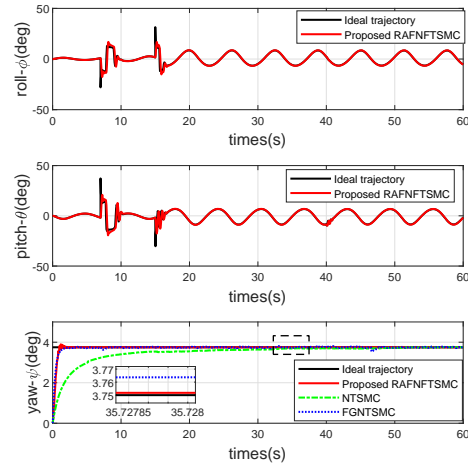
(a) 3-D tracking.



(b) Adaptive gains in case 2.

Figure 8. Tracking and adaptive gains in case 2.

(a) Position tracking.



(b) Attitude tracking.

Figure 9. Tracking performance in case 2.

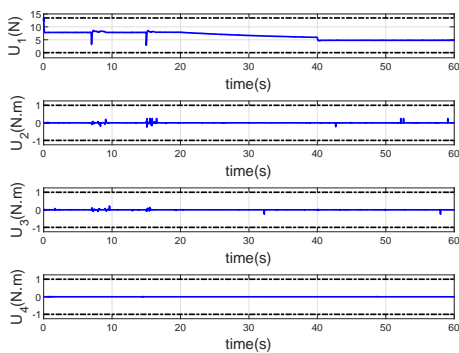
the arctangent nonsingular terminal sliding surface yields finite convergence of the state vectors. The stability of the system has been confirmed by using Lyapunov direct theory. The problem of actuator saturation and time-varying uncertainty are solved by the RAFNFTSMC method in face of random unknown disturbances. To prove the superiority of the RAFNFTSMC proposed in this paper, the simulation results are compared with NTSMC and FGNTSMC schemes. Overall, the results suggest that the proposed RAFNFTSMC can track complex paths fast and precisely, and has a strong anti-chattering ability.

Acknowledgements

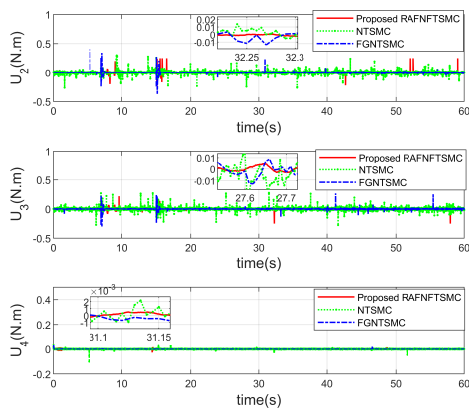
This work is supported in part by the National Natural Science Foundation of China (Grant number: 62003103).

Declaration of conflicting interests

Authors declare that they have no conflict of interest.



(a) Control inputs.



(b) Control inputs comparison.

Figure 10. Control inputs in case 2.

Funding

The presented work is supported by the National Natural Science Foundation of China (Grant number: 62003103).

References

- Shahhatreh H, Sawalmeh AH, Al-Fuqaha A et al. Unmanned aerial vehicles UAVs: A survey on civil applications and key research challenges. *IEEE Access* 2019; 7: 48572–48634.
- Qi Y, Zhu Y, Wang J et al. Mude-based control of quadrotor for accurate attitude tracking. *Control Engineering Practice* 2021; 108: 104721.
- Wang N, Deng Q, Xie G et al. Hybrid finite-time trajectory tracking control of a quadrotor. *ISA transactions* 2019; 90: 278–286.
- Yang Y and Yan Y. Attitude regulation for unmanned quadrotors using adaptive fuzzy gain-scheduling sliding mode control. *Aerospace Science and Technology* 2016; 54: 208–217.
- Hua C, Chen J and Guan X. Adaptive prescribed performance control of QUAVs with unknown time-varying payload and wind gust disturbance. *Journal of the Franklin Institute* 2018; 355(14): 6323–6338.
- Yu H, Yao H, Li Y et al. An interacting control method for quadrotor based on adrc. In *2019 Chinese Control Conference (CCC)*. IEEE, pp. 4783–4788.
- Utkin V. Variable structure systems with sliding modes. *IEEE Transactions on Automatic control* 1977; 22(2): 212–222.
- Chen B, Hu J, Zhao Y et al. Finite-time observer based tracking control of uncertain heterogeneous underwater vehicles using adaptive sliding mode approach. *Neurocomputing* 2022; 481: 322–332.
- Li Y and Wang D. Servo motor sliding mode control based on fuzzy power index method. *Computers & Electrical Engineering* 2021; 94: 107351.
- Yogi S, Tripathi V and Behera L. Adaptive integral sliding mode control using fully connected recurrent neural network for position and attitude control of quadrotor. *IEEE Transactions on Neural Networks and Learning Systems* 2021; 32(12): 5595–5609.
- Nekoukar V and Dehkordi NM. Robust path tracking of a quadrotor using adaptive fuzzy terminal sliding mode control. *Control Engineering Practice* 2021; 110: 104763.
- Oliva-Palomo F, Muñoz-Vázquez AJ, Sánchez-Orta A et al. A fractional nonlinear pi-structure control for robust attitude tracking of quadrotors. *IEEE Transactions on Aerospace and Electronic Systems* 2019; 55(6): 2911–2920.
- Mofid O, Mobayen S, Zhang C et al. Desired tracking of delayed quadrotor UAV under model uncertainty and wind disturbance using adaptive super-twisting terminal sliding mode control. *ISA transactions* 2022; 123: 455–471.
- Xu LX, Ma HJ, Guo D et al. Backstepping sliding-mode and cascade active disturbance rejection control for a quadrotor UAV. *IEEE/ASME Transactions on Mechatronics* 2020; 25(6): 2743–2753.
- Lian S, Meng W, Lin Z et al. Adaptive attitude control of a quadrotor using fast nonsingular terminal sliding mode. *IEEE Transactions on Industrial Electronics* 2021; 69(2): 1597–1607.
- Labbadi M and Cherkaoui M. Robust adaptive nonsingular fast terminal sliding-mode tracking control for an uncertain quadrotor UAV subjected to disturbances. *ISA transactions* 2020; 99: 290–304.
- Wang H, Ye X, Tian Y et al. Model-free-based terminal SMC of quadrotor attitude and position. *IEEE Transactions on Aerospace and Electronic Systems* 2016; 52(5): 2519–2528.
- Eltayeb A, Rahmat MF, Eltoum MM et al. Adaptive fuzzy gain scheduling sliding mode control for quadrotor UAV systems. In *2019 8th International Conference on Modeling Simulation and Applied Optimization (ICMSAO)*. IEEE, pp. 1–5.
- Wang LX. Fuzzy systems are universal approximators. In *1992 Proceedings IEEE International Conference on Fuzzy Systems*. IEEE, pp. 1163–1170.
- Wang Y, Feng Y, Zhang X et al. A new reaching law for antidisruption sliding-mode control of PMSM speed regulation system. *IEEE Transactions on Power Electronics* 2019; 35(4): 4117–4126.
- Shao K, Zheng J, Huang K et al. Finite-time control of a linear motor positioner using adaptive recursive terminal sliding mode. *IEEE Transactions on Industrial Electronics* 2019; 67(8): 6659–6668.